View Article Online / Journal Homepage / Table of Contents for this issue

Synthesis and applications of main-chain Ru(II) metallo-polymers containing bis-terpyridyl ligands with various benzodiazole cores for solar cells†

Harihara Padhy,[a] Duryodhan Sahu,[a] I-Hung Chiang,[a] Dhananjaya Patra,[a] Dhananjay Kekuda,[b] Chih-Wei Chu[bc] and Hong-Cheu Lin*[a]

Received 4th August 2010, Accepted 7th October 2010
DOI: 10.1039/c0jm02532a

Published on 29 November 2010. Downloaded by National Chiao Tung University on 25/04/2014 02:48:02.

A series of π-conjugated bis-terpyridyl ligands (**M1–M3**) bearing various benzodiazole cores and their corresponding main-chain Ru(II) metallo-polymers were designed and synthesized. The formation of metallo-polymers were confirmed by NMR, relative viscosity, and UV-visible titration measurements. The effects of electron donor and acceptor interactions on their thermal, optical, electrochemical, and photovoltaic properties were investigated. Due to the strong intramolecular charge transfer (ICT) interaction and metal to ligand charge transfer (MLCT) in Ru(II)-containing polymers, the absorption spectra covered a broad range of 260–750 nm with the optical band gaps of 1.77–1.63 eV. In addition, due to the broad sensitization areas of the metallo-polymers, their bulk heterojunction (BHJ) solar cell devices containing [6,6]-phenyl-C_{61}-butyric acid methyl ester (PCBM) as an electron acceptor exhibited a high short-circuit current (J_{sc}). An optimum PVC device based on the blended polymer **P1** : PCBM = 1 : 1 (w/w) achieved the maximum power conversion efficiency (PCE) value up to 0.45%, with V_{oc} = 0.61 V, J_{sc} = 2.18 mA cm^{-2}, and FF = 34.1% (under AM 1.5 G 100 mW cm^{-2}), which demonstrated a novel family of conjugated polyelectrolytes with the highest PCE value comparable with BHJ solar cells fabricated from ionic polythiophene and C_{60}.

Introduction

In the extensive search of new materials for optoelectronics applications, supramolecular metallo-polymers have gained much interest in last decades.[1–3] The self-recognition and self-assembly of functional structures into supramolecular metallo-architectures through the interactions of transition metal ions and appropriate chelating ligands has afforded many intriguing architectures that have attained much attention in modern supramolecular chemistry.[4,5] Polypyridyl ligands, especially 2,2′:6′,2″-terpyridine (terpy) derivatives, which have high binding affinities towards transition-metal ions due to dπ–pπ* back-bonding of metal ions to pyridine rings have been utilized recently for multinuclear supramolecular interactions.[6] Terpy derivatives bearing π-conjugated substituents at the 4′-position possess fascinating photophysical, electrochemical, catalytic, and magnetic properties with promising applications in the field of self-assembled molecular devices and photoactive molecular wires,[7] and their properties can be tuned by varying substituents at the 4′-position of the terpy moieties.[8] Furthermore, chemically and thermally stable ditopic bis-terpyridine derivatives, where two terpy units are linked back-to-back with a covalent bond through a spacer, are able to form stable complexes with a large variety of transition-metal ions for the design of functional materials.[9] Three chelating pyridyl units in terpy ligands offer higher binding constants and the formation of distorted octahedral 2 : 1 ligand–metal complexes. In particular, by the proper selection of metal–ligand combinations, it is possible to realize the formation of ligand–metal complexes from kinetically labile to inert but nevertheless thermodynamically stable bonds.

Constable *et al.* have developed the concept concerning the utilization of ditopic bis-terpyridyl ligands as building blocks for coordination oligomers and polymers.[10] By coordinating to suitable metal ions, the electronic properties of these materials can be tuned and that highlights their potential in the applications of new functional materials.[11,12] In the past years, a large number of terpy complexes containing heavy transition metal ions, such as ruthenium(II), iridium(III), or osmium(II), as photoactive species, and also coordination polymers built up from terpy ligands have been introduced by several research groups.[9,13] Zinc(II) ions have also recently attracted much interest as novel templates for the fabrication of structurally well-defined photoluminescent and electroluminescent supramolecular metallocycles and metallo-polymers.[14,15] In our previous reports,[15] a series of terpyridyl Zn(II) metallo-polymers containing polyfluorene backbones as emitters were fabricated into PLED devices with multilayer structures.

Nowadays, some terpyridyl Ru(II) complexes have attracted researchers to use them in the application of photovoltaic cells (PVC).[16,17] The insertion of ruthenium metals into conjugated backbones has several advantages, such as facilitating the charge generation by extending its absorption range due to its characteristic long-lived metal to ligand charge transfer (MLCT)

[a]*Department of Materials Science and Engineering, National Chiao Tung University,Hsinchu, Taiwan, ROC. E-mail: linhc@cc.nctu.edu.tw; Fax: +8863-5724727; Tel: +8863-5712121 ext.55305*
[b]*Research Center for Applied Sciences, Academia Sinica, Taipei, Taiwan, ROC*
[c]*Department of Photonics, National Chiao Tung University, Hsinchu, Taiwan, ROC*

† Electronic Supplementary Information (ESI) available: Experimental details and characterization of aromatic dibromides **5a–5c**, bis-terpyridyl ligands **M1–M3** and metallo-polymers **P1–P3**, including reaction schemes, structures, and figures showing NMR, UV-Visible titrations. See DOI: 10.1039/c0jm02532a

 This journal is © The Royal Society of Chemistry 2011

View Article Online

Published on 29 November 2010. Downloaded by National Chiao Tung University on 25/04/2014 02:48:02.

transition[9d] and to exhibit a reversible Ru(II,III) redox process along with some ligand-centered redox processes. Motivations for examining the potential incorporation of such conjugated polyelectrolytes into solar cell development include the easy processability, layer-by-layer (LBL) processing capability, and the fact that their applications in a variety of chemical and sensory schemes have shown that they are efficiently quenched by electron acceptors. Dye-sensitized solar cells (DSSCs) based on such complexes have also been fabricated and the power conversion efficiency (PCE) values in excess of 10% have been achieved when liquid electrolytes were used.[18] However, the presence of liquid electrolytes inside DSSCs seriously limits the industrial development of the technology due to the poor long-term stabilities of liquid cells. Recently, terpyridyl Ru(II) complexes have been utilized in bulk heterojunction (BHJ) PVC devices by using LBL self-assembled techniques. Chan *et al.* reported that the use of a terpyridyl Ru(II) complex containing conjugated polymer (Ru–PPV) and sulfonated polyaniline (SPAN) for the fabrication of different multilayer PVCs by the LBL deposition method. The short-circuit currents in the PVC devices were measured *ca.* 7.5–32.9 μA cm^{-2} and the PCE values were in the range of 0.95–4.4 × 10^{-3}%.[17a] They also synthesized conjugated polymers with pendant Ru(II) terpyridine trithiocyanato complexes and applied them in bulk heterojunction photovoltaic cells with high PCE values *ca.* 0.12%.[16a] Similarly, Mikroyannidis *et al.* used metallo-polymers in bulk heterojunction photovoltaic cells as a buffer layer along with an active layer of polymer blend P3HT : PCBM (1 : 1 w/w) and found the maximum power conversion efficiency value of 0.71% among the four metallo-polymers studied.[16c] In all cases, the PCE values were limited either by the low open-circuit voltage (V_{oc}) or low short circuit current (J_{sc}). Due to relatively high HOMO levels and reduced sensitization ranges in all the reported polymers, inefficient photocurrents were generated which probably affected their PCE values.

One of the feasible solutions to conquer these problems, *i.e.* to get a higher V_{oc} value and a more favorable overlap of the absorption spectra from both active layer and solar emission, is to introduce electron donor–acceptor structures to the cores of bis-terpyridyl ligands. By choosing different electron donors and acceptors, their absorption edges can be extended due to the intramolecular charge transfer (ICT) between them and also the energy band structures, *i.e.*, highest occupied molecular orbital (HOMO) and lowest unoccupied molecular orbital (LUMO) levels, of these materials can be tuned. The incorporation of the thiophene donor units with benzodiazole acceptor units at the cores of bis-terpyridyl ligands in Ru(II)-containing metallo-polymers to have better photophysical, electrochemical, and photovoltaic properties are very intriguing and thus to motivate this study. Here, we report the design, synthesis, properties, and device applications of Ru(II)-containg metallo-polymers (**P1–P3**) containing donor–acceptor (D–A) bis-terpyridyl ligands bearing different benzodiazole acceptors, including benzothiadiazole, benzoselenodiazole, and benzoxadiazole cores sandwiched between symmetrical thiophene and terpyridyl units. By introducing such D–A structures, broad absorption ranges *ca.* 300–750 nm and ideal HOMO/LUMO levels of the metallo-polymers were obtained. The effects of their donor–acceptor strengths on the electronic and optoelectronic properties were also investigated. In addition, the PVC devices fabricated by these bis-terpyridyl ligands (**M1–M3**) and metallo-polymers (**P1–P3**) with [6,6]-phenyl-C_{61}-butyric acid methyl ester (PCBM) inserted between a transparent anode (ITO/PEDOT:PSS) and a cathode (Ca) were explored, and all photovoltaic parameters obtained are also comparable with the BHJ solar cells fabricated from ionic polythiophene and C_{60}.[19]

Experimental

Materials

All chemicals and solvents were reagent grade and purchased from Aldrich, ACROS, Fluka, TCI, TEDIA, and Lancaster Chemical Co. Toluene, tetrahydrofuran, and diethyl ether were distilled over sodium/benzophenone to keep them anhydrous before use. Chloroform ($CHCl_3$) was purified by refluxing with calcium hydride and then distilled. If not otherwise specified, the other solvents were degassed by nitrogen 1 h prior to use.

Measurements and Characterization

^{1}H NMR spectra were recorded on a Varian Unity 300 MHz spectrometer using $CDCl_3$ and DMSO-d_6 solvents. Elemental analyses were performed on a HERAEUS CHN-OS RAPID elemental analyzer. Thermogravimetric analyses (TGA) were conducted with a TA Instruments Q500 at a heating rate of 10 °C min^{-1} under nitrogen. Viscosity measurements were conducted using 10% weight of metallo-polymer solutions (in NMP) and compared to measurements made on bis-terpyridyl ligand solutions under the same condition (with viscosity η = 6 cp) on a BROOKFILEL DV-III+ RHEOMETER system at 25 °C (100 RPM, Spindle number 4). UV-visible absorption spectra were recorded in dilute chloroform (for **M1–M3**) and DMF (for **P1–P3**) solutions (10^{-6} M) on a HP G1103A spectrophotometer. The solid films for the solid-state UV-vis measurements were spin-coated on quartz substrates from chloroform and DMF solutions with a concentration of 10 mg mL^{-1} of the bis-terpyridyl ligands (**M1–M3**) and polymers (**P1–P3**), respectively. UV-vis titrations were performed by taking 10^{-5} M of bis-terpyridyl ligands (**M1–M3**) in the co-solvent of chloroform : acetonitrile (8 : 2 v/v), and titrated with 50 μL aliquots of 3.9 × 10^{-4} M solutions containing metal salts $Zn(OAc)_2$ in EtOH. Cyclic voltammetry (CV) measurements were performed using a BAS 100 electrochemical analyzer with a standard three-electrode electrochemical cell in a 0.1 M tetrabutylammonium hexafluorophosphate (Bu_4NPF_6) solution (in acetonitrile) at room temperature with a scanning rate of 100 mV s^{-1}. During the CV measurements, the solutions were purged with nitrogen for 30 s. In each case, a carbon working electrode coated with a thin layer of monomers or polymers, a platinum wire as the counter electrode, and a silver wire as the quasi-reference electrode were used, and Ag/AgCl (3 M KCl) electrode was served as a reference electrode for all potentials quoted herein. The redox couple of ferrocene/ferrocenium ion (Fc/Fc^+) was used as an external standard. The corresponding HOMO and LUMO levels were calculated using $E_{ox/onset}$ and $E_{red/onset}$ for experiments in solid films, which were performed by drop-casting films with similar thicknesses from THF or DMF solutions (*ca.* 5 mg mL^{-1}).

View Article Online

Published on 29 November 2010. Downloaded by National Chiao Tung University on 25/04/2014 02:48:02.

Fabrication of PVC device

The photovoltaic (PV) cells in this study were composed of an active layer of blended bis-terpyridyl ligands (**M1–M3**) or metallo-polymers (**P1–P3**) with [6,6]-phenyl-C_{61}-butyric acid methyl ester (PCBM) in solid films, which were sandwiched between a transparent indium tin oxide (ITO) anode and a metal cathode. Prior to the device fabrication, ITO-coated glass substrates (1.5 × 1.5 cm) were ultrasonically cleaned in detergent, deionized water, acetone, and isopropyl alcohol sequentially. After routine solvent cleaning, the substrates were treated with UV ozone for 15 min. Then, a modified ITO surface was obtained by spin-coating a layer of poly(ethylene dioxythiophene): polystyrenesulfonate (PEDOT:PSS) (~30 nm thick). After baking at 130 °C for one hour, the substrates were transferred to a nitrogen-filled glove box. The PVC devices were fabricated by spin-coating solutions of blended bis-terpyridyl ligands (**M1–M3**) or metallo-polymers (**P1–P3**):PCBM (1 : 1 w/w) onto the PEDOT:PSS modified substrates at 1500 rpm for 60 s (*ca.* 100 nm), and placed in a covered glass Petri dish. Initially, the blended solutions were prepared by dissolving both bis-terpyridyl ligands (**M1–M3**) and PCBM (1 : 1 w/w) in chloroform (20 mg mL^{-1}) and both metallo-polymers (**P1–P3**) and PCBM (1 : 1 w/w) in DMF (20 mg mL^{-1}), and followed by continuous stirring for 12 h at 50 °C. Finally, a calcium layer (30 nm) and a subsequent aluminium layer (100 nm) were thermally evaporated through a shadow mask at a pressure below 6×10^{-6} Torr, where the active area of the device was 0.12 cm^2. All PVC devices were prepared and measured under ambient conditions. The solar cell testing was done inside a glove box under simulated AM 1.5G irradiation (100 mW cm^{-2}) using a Xenon lamp based solar simulator (Thermal Oriel 1000W). The light source was a 450 W Xe lamp (Oriel Instrument, model 6266) equipped with a water-based IR filter (Oriel Instrument, model 6123NS). The light output from the monochromator (Oriel Instrument, model 74100) was focused onto the photovoltaic cell under test.

General synthetic procedure for bis-terpyridyl ligands (M1–M3)

M1–M3 were prepared *via* a Stille coupling reaction using tetrakis(triphenylphosphine)palladium as a catalyst. In a flame dried two-neck flask, 1.00 eq. of dibromo compounds (**5a–5c**) and 2.50 eq. of compound **2** in toluene were degassed with Argon. Then, 0.03 eq. $Pd(PPh_3)_4$ was added and refluxed for 2 days. The reaction mixtures were cooled to room temperature, and the solvents were removed by reduced pressure. After removal of the solvents, the product was precipitated from methanol. Further purification was achieved by column chromatography on alumina with chloroform as an eluant to give the products.

M1. According to the above-mentioned general procedure, **M1** was obtained as a purple solid (yield: 68%). ^{1}H NMR ($CDCl_3$, 300 MHz, δ): 8.77 (d, $J = 4.2$ Hz, 4H), 8.63 (m, 8H), 7.91 (s, 2H), 7.85 (dd, $J = 7.8$ Hz, $J = 1.8$ Hz, 4H), 7.72 (S, 2H), 7.69 (d, $J = 3.9$ Hz, 2H), 7.35 (dd, $J = 7.8$ Hz, $J = 1.8$ Hz, 4H), 7.22 (d, $J = 3.9$ Hz, 2H), 2.87(t, $J = 6.9$ Hz, 4H), 1.75 (m, 4H), 1.40–1.29 (m, 12H), 0.93 (t, $J = 5.4$ Hz, 6H). ^{13}C NMR ($CDCl_3$, 75 MHz, δ): 156.29, 149.43, 149.35, 143.29, 141.28, 138.26, 137.10, 132.95, 132.09, 130.91, 129.51, 128.83, 126.60, 125.47, 124.16, 121.54, 117.84, 116.94, 31.96, 30.69, 29.98, 29.55, 22.90, 14.36. MS (FAB): *m/z* [M+] 1096; calcd *m/z* [M+] 1095.49. Element anal. calcd for $C_{64}H_{54}N_8S_5$: C, 70.17; H, 4.97; N, 10.23; found: C, 69.51; H, 5.26; N, 10.15.

M2. According to the above-mentioned general procedure, **M2** was obtained as a black solid (yield: 63%). ^{1}H NMR ($CDCl_3$, 300 MHz, δ): 8.74 (d, $J = 4.2$ Hz, 4H), 8.61 (m, 8H), 7.85 (dd, $J = 7.8$ Hz, $J = 1.8$ Hz, 4H), 7.78 (s, 2H), 7.67 (d, $J = 3.9$ Hz, 2H), 7.62 (s, 2H), 7.35 (dd, $J = 7.8$ Hz, $J = 1.8$ Hz, 4H), 7.19 (d, $J = 3.6$ Hz, 2H), 2.84 (t, $J = 6.9$ Hz, 4H), 1.74 (m, 4H), 1.40–1.29 (m, 12H), 0.93 (t, $J = 5.4$ Hz, 6H). ^{13}C NMR ($CDCl_3$, 75 MHz, δ): 158.41, 156.22, 149.31, 143.22, 141.15, 140.79, 138.44, 137.83, 137.05, 132.93, 130.51, 127.98, 126.54, 125.44, 124.11, 121.67, 117.84, 116.88, 31.99, 30.63, 29.98, 29.61, 22.93, 14.39. MS (FAB): *m/z* [M+] 1143; calcd *m/z* [M+] 1142.39. Element anal. calcd for $C_{64}H_{54}N_8S_4Se$: C, 67.29; H, 4.76; N, 9.81; found: C, 66.77; H, 5.30; N, 9.63.

M3. According to the above-mentioned general procedure, **M3** was obtained as a dark purple solid (yield: 76%). ^{1}H NMR ($CDCl_3$, 300 MHz, δ): 8.75 (d, $J = 4.2$ Hz, 4H), 8.69 (m, 8H), 7.96 (s, 2H), 7.87 (dd, $J = 7.2$ Hz, $J = 1.8$ Hz, 4H), 7.73 (d, $J = 3.6$ Hz, 2H), 7.50 (s, 2H), 7.37 (dd, $J = 6.9$ Hz, $J = 1.2$ Hz, 4H), 7.25 (d, $J = 3.9$ Hz, 2H), 2.88 (t, $J = 7.2$ Hz, 4H), 1.78 (m, 4H), 1.40–1.29 (m, 12H), 0.93 (t, $J = 6.9$ Hz, 6H). ^{13}C NMR ($CDCl_3$, 75 MHz, δ): 155.72, 148.96, 148.35, 143.10, 141.16, 138.10, 137.36, 133.05, 132.09, 130.68, 129.41, 128.63, 126.85, 125.28, 122.94, 121.61, 117.69, 116.97, 31.98, 30.60, 30.03, 29.60, 22.94, 14.38. MS (FAB): *m/z* [M+] 1078; calcd *m/z* [M+] 1078.33. Element anal. calcd for $C_{64}H_{54}N_8S_4O$: C, 71.21; H, 5.04; N, 10.38; found: C, 70.75; H, 5.21; N, 10.11.

General synthetic procedure for metallo-polymers (P1–P3)

In a flame dried flask, a mixture of $RuCl_3 \cdot 3H_2O$ (0.11 mmol) and $AgBF_4$ (0.38 mmol) was refluxed for 2 h in acetone (15 mL). After cooling to room temperature, the precipitated AgCl was filtered off, and the obtained solution was evaporated to dryness. The remaining solid was redissolved in *n*-butanol (15 mL), and to this solution, bis-terpyridyl ligand **M1**, **M2**, or **M3** (0.1 mmol) was added, and the resulting solution was refluxed for 5 days. As soon as the precipitation of the formed polymer was observed, a small portion of DMA was added to the mixture (Σ ≈ 20 mL) to redissolve the product. Finally, an excess of NH_4PF_6 (50 mg in 20 mL DMA) was added to the hot solution and stirring was continued for 1 h. The resulting solution was poured dropwise into methanol (200 mL). The precipitated metallo-polymer product was filtered off and washed with methanol (200 mL). Further purification was achieved by repetitively dissolving the metallo-polymer in NMP (2 mL) followewd by precipitation from diethyl ether. Finally, the products were dried under vacuum at 40 °C for 24 h.

P1. According to the above-mentioned procedure, metallo-polymer **P1** was obtained as a dark solid (yield: 66%). ^{1}H NMR (DMSO-d_6, 300 MHz, δ): 9.36 (br, 4H), 9.12 (br, 4H), 8.52 (br, 2H), 8.24 (br, 8H), 7.67 (br, 6H), 7.31 (br, 4H), 3.05 (br, 4H), 1.86 (br, 4H), 1.25–1.40 (br, 12H), 0.92 (br, 6H).

P2. According to the above-mentioned procedure, metallo-polymer **P2** was obtained as a dark solid (yield: 58%). ^{1}H NMR (DMSO-d_6, 300 MHz, δ): 9.36 (br, 4H), 9.12 (br, 4H),

 This journal is © The Royal Society of Chemistry 2011

View Article Online

Published on 29 November 2010. Downloaded by National Chiao Tung University on 25/04/2014 02:48:02.

8.48 (br, 2H), 8.14 (br, 8H), 7.68 (br, 6H), 7.30 (br, 4H), 3.08 (br, 4H), 1.83 (br, 4H), 1.20–1.53 (br, 12H), 0.91 (br, 6H).

P3. According to the above-mentioned procedure, metallo-polymer **P3** was obtained as a dark solid (yield: 77%). ^{1}H NMR (DMSO-d_6, 300 MHz, δ): 9.39 (br, 4H), 9.13 (br, 4H), 8.54 (br, 2H), 8.10 (br, 8H), 7.65 (br, 6H), 7.33 (br, 4H), 2.94 (br, 4H), 1.83 (br, 4H), 1.20–1.53 (br, 12H), 0.89 (br, 6H).

Results and discussion

Synthesis and structural characterization

The general synthetic routes of ditopic bis-terpyridyl ligands (**M1–M3**) and metallo-polymers (**P1–P3**) are shown in Scheme 1. The ditopic bis-terpyridyl monomers in which, acceptor spacer units sandwiched in between two hexyl thiophene units were synthesized in multistep procedures. Detail synthesis and characterization are described in the supporting information.† 4′-(2-Bromo-5-thienyl)-2,2′,6′,2″-terpyridine (**1**) was prepared by the modified method described in the literature,[7f] then tributyltin group was introduced using a palladium(0) catalyzed reaction of compound **1** with excess bis-(tributyltin). Hexyl-thiophene units were added to both sides of each acceptor units through the Suzuki coupling reaction between 2-(4-hexylthiophen-2-yl)-4,4,5,5-tetramethyl-1,3,2-dioxaborolane (**2**) and dibromo arenes (**3a–3c**) in the presence of a catalyst $Pd(PPh_3)_4$. Then these compounds were brominated with NBS to produce compounds **5a–5c**. The aromatic dibromides **5a–5c** were reacted with two equivalents of 4′-(5-tributylstannanyl-thiophen-2-yl)-[2,2′;6′,2″]terpyridine (**2**) under Pd^0-catalyzed Stille cross-coupling conditions to form ditopic bis-terpyridyl ligands (**M1–M3**). After precipitation from methanol and column chromatographic purification, the bis-terpyridyl ligands (**M1–M3**) were obtained in moderate to good yields and fully characterized by ^{1}H NMR, ^{13}C NMR, MS spectroscopy, and elemental analysis.

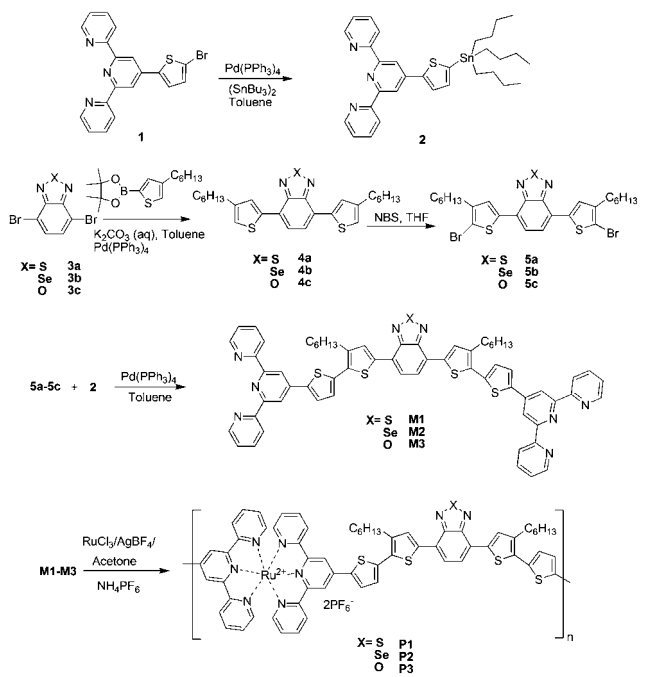

Scheme 1 Synthetic route for bis-terpyridyl ligands (**M1–M3**) and Ru(II)-containing metallo-polymers (**P1–P3**).

The synthesis of Ru(II)-based metallo-polymers (**P1–P3**) is also depicted in Scheme 1. The metallo-polymerization by self-assembly was carried out according to the methods described in the literature.[13e] In a typical polymerization process, an appropriate quantity of ruthenium trichloride was activated by de-chlorinating with $AgBF_4$ in acetone. The resulting hexa-acetone Ru(III) complex was reacted with exactly 1 equiv. of bis-terpyridyl ligands **M1–M3** in *n*-butanol/DMA for 5 days, which involved a reduction of Ru(III) to Ru(II) with the chain growth process using the *n*-butanol solvent itself as a reducing agent. The resulting metallo-polymers (**P1–P3**) were purified by repetitive precipitation from NMP in diethyl ether and dried in vacuum, leading to homopolymers **P1–P3** (yield: 58–78%). The resulting highly linear rigid polymer containing charged metal ions exhibited reduced solubility in common organic solvents as compared with the terpyridyl ligands **M1–M3**, but were soluble in highly polar aprotic solvents, *e.g.*, DMSO, DMF, NMP, or DMA.

Fig. 1 shows ^{1}H NMR spectra in the aromatic regions of ligands and metallo-polymers. As a result of metallo-polymerization, broadened signals of bis-terpyridyl ligands, as well as the absence of the signals from the uncomplexed terpyridyl units were observed. Furthermore, clear and dramatic downfield shifts of the (5,5″)-, (4,4″)-, (3,3″)-, and (3′,5′)-terpyridyl signals and upfield shifts of the (6,6″)- signals were observed upon polymerization, which are consistent with the reported literature.[20] The assignments of terpyridyl signals are shown in Fig. 1 based on those reported for Ru(II) model complexes.[13] Due to the lack of end group-signals in the ^{1}H NMR spectra and also considering the limit of NMR spectroscopy, the formation of cyclic oligomers can be discarded and the synthesized metallo-polymers should consist of more than 30 repeating units.[13e] Hence, the molar masses of **P1–P3** were estimated to be higher than 30000 g mol^{-1}. To further confirm the formation of supramolecular metallo-polymers, the relative viscosity measurements of

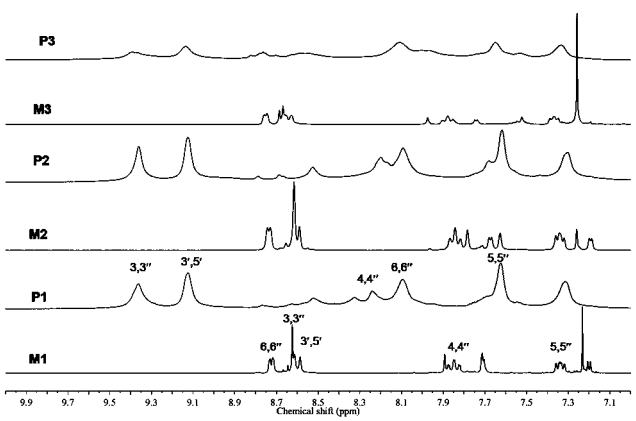

Fig. 1 ^{1}H NMR spectra (aromatic region) of bis-terpyridyl ligands **M1–M3** (in $CDCl_3$) and metallo-polymers **P1–P3** (in DMSO-d_6). The signals belonging to the terpyridyl moiety are assigned in the representative ligand **M1** and polymer **P1**, and the other signals correspond to the π-conjugated spacer. For all spectra: 300 MHz, room temperature.

View Article Online

Published on 29 November 2010. Downloaded by National Chiao Tung University on 25/04/2014 02:48:02.

polymers to bis-terpyridyl ligands were evaluated. For this purpose, solutions of bis-terpyridyl ligands **M1–M3** (10 wt%) in NMP with viscosities η = 6–7 cp at 25 °C were taken as references to dertermine the viscosities of the metallo-polymers (**P1–P3**). As shown in Table 1, **P1–P3** (with η = 9–11 cp) exhibited viscosity 1.50–1.66 times larger than their corresponding bis-terpyridyl ligands **M1–M3**, which is in good agreement with similar reports known from the literature.[11f,15,21]

The thermal properties of the bis-terpyridyl ligands **M1–M3** and metallo-polymers **P1–P3** were determined by thermogravimetric analysis (TGA) at a heating rate of 10 °C min^{-1} under nitrogen and are shown in Fig. 2 and summarized in Table 1. The TGA thermograms revealed decomposition temperatures (T_d) (5% weight loss) of the bis-terpyridyl ligands and polymers were in the range of 369–404 and 431–438 °C, respectively. All bis-terpyridyl ligands and polymers demonstrated the same appearance of two degradation temperatures. In contrast to bis-terpyridyl ligands, polymers exhibited slightly enhanced thermal stability due to the increased rigidity of main-chain structures in metallo-polymers.

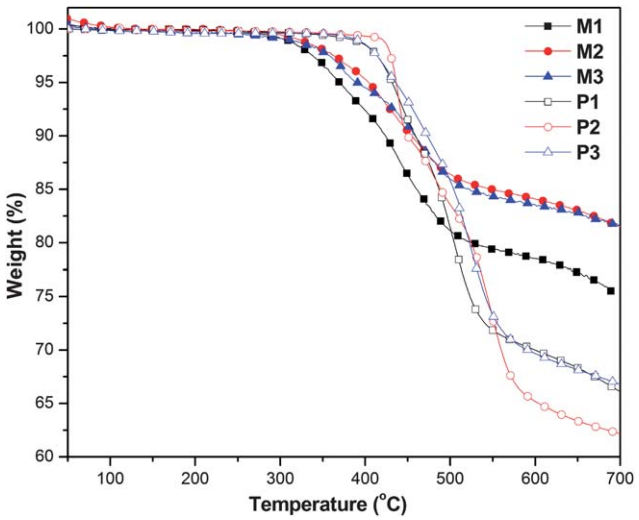

Fig. 2 TGA thermograms of bis-terpyridyl ligands (**M1–M3**) and metallo-polymers (**P1–P3**) at a heating rate of 10 °C min^{-1} under nitrogen.

UV-visible titration

UV-vis titration experiments were carried out to verify the formation of metallo-polymers from bis-terpyridyl ligands (**M1–M3**). As kinetic studies by titration are too slow to detect Ru(II)-containing metallo-polymers, which require heat and relatively long reaction times, these techniques could not be applied to the development of **P1–P3**. In our previous reports, ^{1}H-NMR and UV-vis absorption titration experiments were proceeded to characterize Zn(II)-based metallo-polymers,[15] where the formation of linear metallo-polymers were controlled by the exact stoichiometric ratios of the metal ions (Zn^{2+}) and bis-terpyridyl ligands. Therefore, the same technique is chosen to gain a further insight into the self-assembly mechanism of **M1–M3** towards metallo-polymers, and the related titration data are depicted in Fig. 3. Upon the stepwise addition of Zn^{2+} to a solution of bis-terpyridyl ligand **M1**, the absorption spectra revealed the gradual emergence of an absorption band at 325 nm along with the disappearance of an absorption band at 380 nm. Furthermore, a red-shifted absorption band *ca.* 280 nm along with two isosbestic points (*ca.* 351 and 416 nm) were observed, which suggests that equilibrium occurred among a finite number of spectroscopically distinct species. The titration curve (Fig. 3, inset) showed a linear increase and a sharp end point at a ratio of 1 : 1 (Zn^{2+}:**M1**), indicating the formation of Zn(II)-based metallo-polymers. New absorption peak observed at 325 nm could be attributed to the intra-ligand charge transfer (ILCT) in Zn(II)-based metallo-polymers.[22] The same trends were observed in the bis-terpyridyl ligands **M2** and **M3** (see the supporting information†). Thus, the results of all the titration experiments performed for bis-terpyridyl ligands (**M1–M3**) with Zn^{2+} ions are consistent with the fact that, at a 1 : 1 ratio of Zn^{2+} ions and the ditopic ligands, supramolecular assemblies of metallo-polymers have formed, where each Zn^{2+} ion is complexed with two bis-terpyridyl ligands, and the resulting repeating unit of bis-terpyridyl-Zn^{2+} in metallo-polymers can be considered as the origin of the observed electronic transitions.

Optical properties

The photophysical characteristics of the bis-terpyridyl ligands (**M1–M3**) and metallo-polymers (**P1–P3**) were investigated by ultraviolet-visible (UV-vis) absorption spectroscopy in dilute solutions (10^{-6} M) and spin-coated films on quartz substrates. Fig. 4 shows the absorption spectra of **M1–M3** and **P1–P3** in

Table 1 Optical, thermal, and viscosity properties of bis-terpyridyl ligands (**M1–M3**) and metallo-polymers (**P1–P3**)

Compound	η/cp[a]	T_d/°C[b]	$\lambda_{abs,sol}$/nm[c]	$\lambda_{abs,film}$/nm[d]	λ_{onset}/nm	E_g^{opt}/eV[e]
M1	7	369	280, 381, 514	285, 415, 566	698	1.77
M2	6	404	281, 396, 553	286, 428, 602	744	1.66
M3	6	401	280, 378, 520	287, 422, 572	702	1.76
P1	11	431	278, 318, 335,550, 576	282, 320, 335, 554, 605	710	1.74
P2	9	438	278, 318, 335, 551, 596	280, 321, 335, 554, 638	761	1.63
P3	10	432	278, 318, 335, 549, 572	282, 321, 335, 554, 606	713	1.73

[a] The viscosities of polymers (10% in weight) in NMP solutions at 25 °C (100 rpm, Spindle number 4) were determined by a rheometer system. Solutions of bis-terpyridyl ligands **M1–M3** (10% in weight) in NMP were used as references to determine the viscosities of the corresponding metallo-polymers. [b] The decomposition temperatures (T_d) (5% weight loss) were determined by TGA with a heating rate of 10 °C min^{-1} under a N_2 atmosphere. [c] Concentration of 10^{-6} M in chloroform for **M1–M3** and 10^{-6} M in DMF for **P1–P3**. [d] Spin coated from solutions on quartz substrates. [e] Optical band gaps were estimated from the absorption spectra in films by using the equation $E_g = 1240/\lambda_{edge}$.

 This journal is © The Royal Society of Chemistry 2011

View Article Online

Published on 29 November 2010. Downloaded by National Chiao Tung University on 25/04/2014 02:48:02.

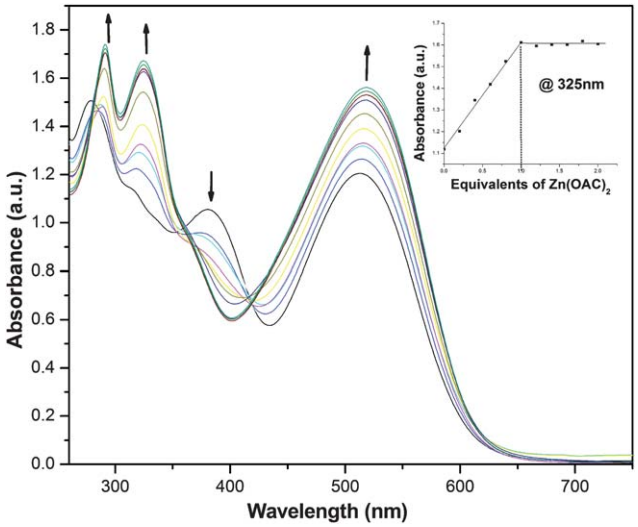

Fig. 3 UV-vis absorption spectra acquired upon the titration of bis-terpyridyl ligand **M1** (in 2 : 8 v/v CH_3CN–$CHCl_3$) with $Zn(OAc)_2$ (in EtOH). The inset shows the normalized absorption at 325 nm as a function of Zn^{2+}:**M1**.

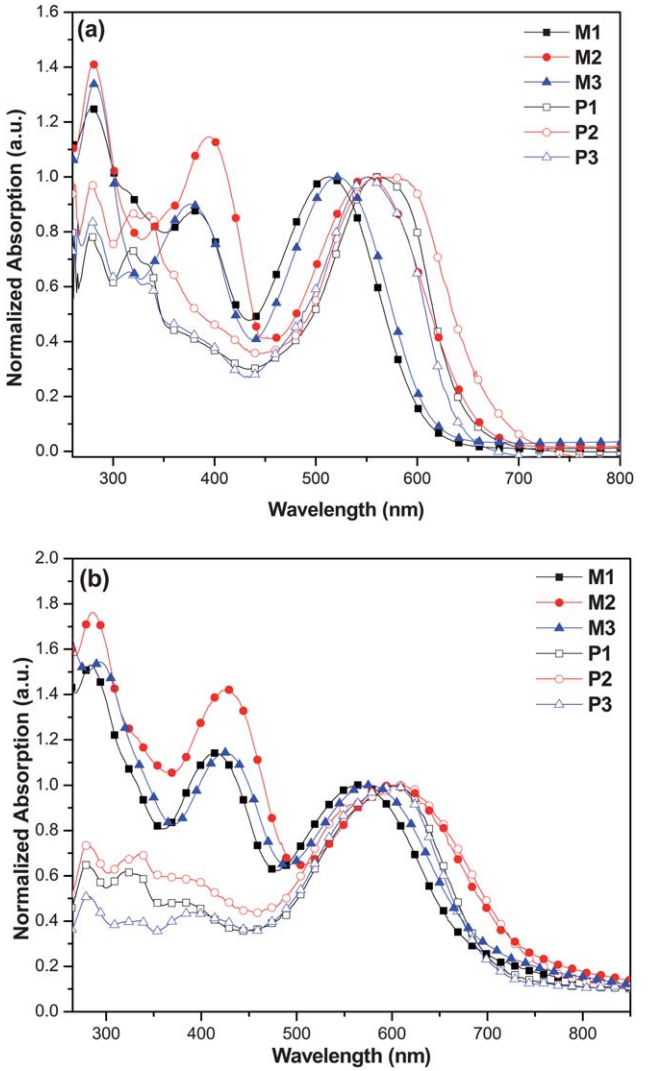

Fig. 4 Normalized UV-vis spectra of bis-terpyridyl ligands (**M1–M3**) and metallo-polymers (**P1–P3**). (a) In dilute (10^{-6} M) solutions and (b) in solid films.

solutions as well as in solid films, and their optical data, including the absorption wavelengths (λ_{abs}) and optical band gaps (E_g^{opt}), are also summarized in Table 1. The absorption spectra of ditopic ligands **M1–M3** showed three intense band regions, where the band *ca.* 280 nm was associated with the characteristic π–π* transitions of the terpyridine moieties[23] and the low energy peaks *ca.* 380 nm and 514–553 nm (with tailing around 700 nm) were due to the π–π* transitions and intramolecular charge transfer (ICT) occurring inside the π-conjugated systems. Compared with solutions, these two longer wavelength bands were red-shifted in the solid films (*ca.* 34 nm and 52 nm, respectively), which could be attributed to the strong interchain associations and aggregations in solids. Due to the larger size and smaller electronegativity of the selenium (Se) atom compared to those of both S and O atoms in benzodiazole acceptors, the bis-terpyridyl ligand **M2** showed the most pronounced bathochromic shift of the absorption maximum and, thereby, a smaller optical energy bandgap (1.66 eV) than the other bis-terpyridyl ligands (1.77 and 1.76 eV for **MI** and **M3**, respectively). In all the bis-terpyridyl ligands, the acceptor moieties are sandwiched between thiophene units, resulting in more planar structures to facilitate inter-chain associations and strong ICT interactions between thiophene donors and benzodiazole acceptors,[24] so their absorption spectra covered a broad range. In contrast to the recently published bis-terpyridyl monomers containing acceptor moieties,[14a] our terpyridyl ligands (**M1–M3**) showed stronger red shifts in the absorption spectra with smaller optical band gaps due to the stronger ICT interactions, which are highly essential for the PVC devices to increase the photo-current generations.

Metal–ligand coordination, *i.e.*, formation of metallo-polymers (**P1–P3**), can also be easily confirmed through UV-vis absorption spectroscopy. In ruthenium-containing metallo-polymers, self-assembly induced by metal ions is readily observed by the occurrence of an additional absorption band (metal-to-ligand charge-transfer, *i.e.*, MLCT) at 490–560 nm,[9d,25] which was derived from the promotion of an electron from the metal (Ru(II))-centered d-orbital to unfilled ligand-centered π* orbitals. All thet hmetallo-polymers **P1–P3**, showed the ligand-centered π–π* transitions between terpy moieties and central chromophores (thiophene donors and benzodiazole acceptors) situated *ca.* λ_{abs} < 350 nm. The metal-to-ligand charge transfer (MLCT) bands were in the range of 550–554 nm in these coordination polymers (**P1–P3**), and a strong bathochromic effect in MLCT was observed due to the presence of benzodiazole acceptors inserted between thiophene units as the central cores.[16e] The absorption peaks beyond 550 nm were attributed to the stronger ICT interactions inside the bis-terpyridyl ligands. It is worth noting that compared with the other Ru(II)-containing metallo-polymers,[9d] our metallo-polymers showed extended absorption beyond MLCT. Due to the long absorption range of these metallo-polymers, they possessed small optical band gaps in the range of 1.63–1.74 eV. Similar to bis-terpyridyl ligands, low

View Article Online

Published on 29 November 2010. Downloaded by National Chiao Tung University on 25/04/2014 02:48:02.

energy absorption wavelengths (λ_{abs}) in solid films (*ca.* 605–638 nm) of metallo-polymers **P1–P3** were red shifted (29–42 nm) in comparison with those in solutions (572–596 nm), which could be also attributed to the strong interchain associations and aggregations in solids. Compared with bis-terpyridyl ligands (**M1–M3**) in both solutions and solid films, the maximum absorption wavelengths (λ_{abs}) of metallo-polymers (**P1–P3**) exhibited stronger bathochromic shifts due to the formation of linear and rigid metallo-polymers.

Electrochemical properties

The redox behavior and electronic states, *i.e.*, HOMO and LUMO levels, of the bis-terpyridyl ligands (**M1–M3**) and their corresponding Ru(II)-containing metallo-polymers (**P1–P3**) were investigated by cyclic voltammetry (CV) measurements to understand the energy band structures of associated materials used in the PVC devices. The cyclic voltammograms of bis-terpyridyl ligands **M1–M3** and metallo-polymers **P1–P3** in solid films are displayed in Fig. 5 and the related CV data (formal potentials, onset potentials, HOMO and LUMO levels, and band gaps) are summarized in Table 2. Ag/AgCl served as the reference electrode and it was calibrated by ferrocene ($E_{1/2(FC/FC^+)}$ = 0.45 eV *versus* Ag/AgCl). The HOMO and LUMO levels were estimated by the oxidation and reduction potentials from the reference energy level of ferrocene (4.8 eV below the vacuum level) according to the following equation:[15] $E_{HOMO}/E_{LUMO} = [-(E_{onset} - E_{onset(FC/FC^+ \textit{ vs. } Ag/Ag^+)}) - 4.8]$ eV where 4.8 eV is the energy level of ferrocene below the vacuum level and $E_{onset(FC/FC^+ \textit{ vs. } Ag/Ag^+)}$ = 0.45 eV. All bis-terpyridyl ligands (**M1–M3**) exhibited two p-doping/dedoping (oxidation/rereduction) processes at positive potentials and one n-doping/dedoping (reduction/reoxidation) process at negative potentials. The onset oxidation potentials ($E_{ox/onset}$) were the same for **M1–M3** *ca.* 0.88 V, and two of their formal oxidation potentials were in the range of 1.05–1.15 V and 1.28–1.34 V. In addition, the onset reduction potentials ($E_{red/onset}$) of **M1–M3** were in the range of (−0.85)–(−0.93) V and their formal oxidation potentials were in the range of (−1.03)–(−1.15) V. From the onset oxidation potentials ($E_{ox/onset}$) and onset reduction potentials ($E_{red/onset}$) of bis-terpyridyl ligands **M1–M3**, the estimated HOMO levels were at *ca.* −5.24 eV and LUMO levels were in the range of (−3.42)–(−3.50) eV. The similar values in the HOMO levels of these ligands suggest that different electron-deficient center units have almost no effect on their oxidation potentials, but the reduction potentials of these ligands behave quite differently. The LUMO levels are clearly affected by the electron-deficient centers of the ligand cores, a stronger electron-deficient unit resulting in a lower LUMO energy level.[24a]

All Ru(II)-containing metallo-polymers (**P1–P3**) exhibited two reversible or quasi-reversible oxidation peaks in the range of 1.00–1.02 V and 1.51–1.57 V, respectively. In agreement with the literature, these waves were attributed to the metal localized oxidation (corresponding to the II/III redox transition) and redox transitions across the bridging ligands, respectively.[17a,26] These polymers also showed one reduction process at *ca.* 1.08 V, which was assigned to the ligand-based reduction.[14a,15] From the onset oxidation potentials ($E_{ox/onset}$, *ca.* 0.77 V) and onset reduction potentials ($E_{red/onset}$, between 0.73 and 0.79 V) of metallo-polymers, the estimated HOMO levels were at *ca.* −5.11 eV and LUMO levels were between −3.56 and −3.62 eV. Apparently, the HOMO levels in these metallo-polymers stayed relatively constant while the LUMO levels were tuned by varying the electron withdrawing aromatic substituents on the bis-terpyridyl ligands.[27] Again, compared with the bis-terpyridyl ligands, the HOMO levels of metallo-polymers were enhanced by *ca.* 0.12 eV. As a result, their band gaps decreased to give narrow-band-gap metallo-polymers. The electrochemical band gaps (E_g^{ec}) calculated from $E_g^{ec} = e(E_{ox/onset} - E_{red/onset})$ were 1.56, 1.49, and 1.54 eV for **P1–P3**, respectively. All these electrochemical characteristics are within the desirable range of ideal materials to be utilized in the organic photovoltaic applications.

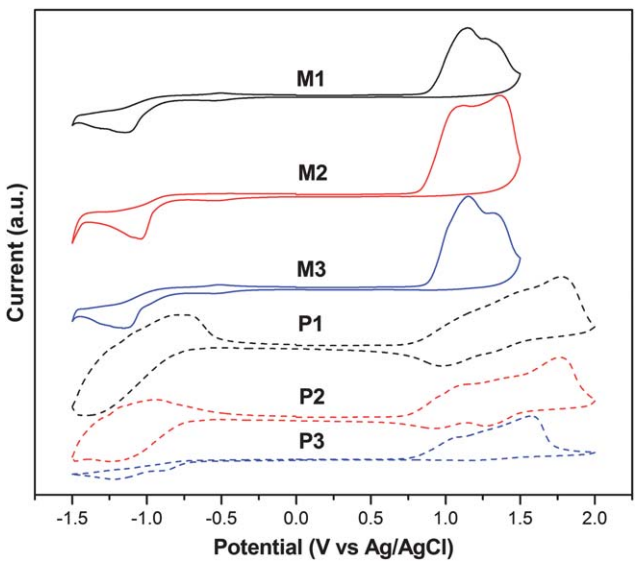

Fig. 5 Cyclic voltammograms of bis-terpyridyl ligands (**M1–M3**) and metallo-polymers (**P1–P3**) at a scan rate of 100 mV s^{-1}.

Photovoltaic properties

To investigate the potential use of bis-terpyridyl ligands **M1–M3** and their Ru(II)-containing metallo-polymers **P1–P3** in PVCs, the bulk hetero-junction (BHJ) solar cell devices comprising blends of these compounds as electron donors and [6,6]-phenyl-C_{61}-butyric acid methyl ester (PCBM) as an electron acceptor in their active layer were fabricated with a configuration of ITO/PEDOT:PSS(30 nm)/**M1–M3** or **P1–P3**:PCBM blend (~80 nm)/Ca(30 nm)/Al(100 nm) and measured under AM 1.5 stimulated solar light. The blended solutions were prepared from compounds and PCBM in a weight ratio of 1 : 1 (w/w) from chloroform solutions of **M1–M3** and from DMF solutions of **P1–P3**. The current density (*J*) *versus* voltage (*V*) curves of the PVCs are shown in Fig. 6, where the open circuit voltage (V_{oc}), short circuit current density (J_{sc}), fill factor (*FF*), and the PCE values are summarized in Table 3. In all PVC devices, the thickness of the active layer was kept at *ca.* 80 nm, which has the optimum performance due to the balance in optical absorption and serial resistance of the blended film.

Among bis-terpyridyl ligands **M1–M3**, the highest PCE value of 0.13% was obtained from the device containing an active layer of **M1**:PCBM (1 : 1 w/w) with V_{oc} = 0.43 V, J_{sc} = 0.97 mA cm^{-2},

 This journal is © The Royal Society of Chemistry 2011

View Article Online

Published on 29 November 2010. Downloaded by National Chiao Tung University on 25/04/2014 02:48:02.

Table 2 Electrochemical properties of bis-terpyridyl ligands (**M1–M3**) and metallo-polymers (**P1–P3**)[a]

Compound	Oxidation potential/V *vs.* Ag/Ag^+		Reduction potential/V *vs.* Ag/Ag^+		Energy level[d]/eV		Band gap/eV	
	$E_{ox/onset}$[b]	$E_{ox/o}$[c]	$E_{red/onset}$[b]	$E_{red/o}$[c]	HOMO	LUMO	E_g^{ec}	E_g^{opt}
M1	0.89	1.15, 1.28	−0.93	−1.12	−5.24	−3.42	1.82	1.77
M2	0.88	1.05, 1.34	−0.85	−1.03	−5.23	−3.50	1.73	1.66
M3	0.89	1.13, 1.31	−0.92	−1.15	−5.24	−3.43	1.81	1.76
P1	0.77	1.01, 1.57	−0.79	−1.08	−5.12	−3.56	1.56	1.74
P2	0.76	1.00, 1.51	−0.73	−1.06	−5.11	−3.62	1.49	1.63
P3	0.77	1.02, 1.57	−0.77	−1.12	−5.12	−3.58	1.54	1.73

[a] Reduction and oxidation potentials measured by cyclic voltammetry in solid films. [b] Onset oxidation and reduction potentials. [c] Formal oxidation and reduction potentials. [d] $E_{HOMO}/E_{LUMO} = [-(E_{onset} - 0.45) - 4.8]$ eV, where 0.45 V is the value for ferrocene *vs.* Ag/Ag^+ and 4.8 eV is the energy level of ferrocene below the vacuum.

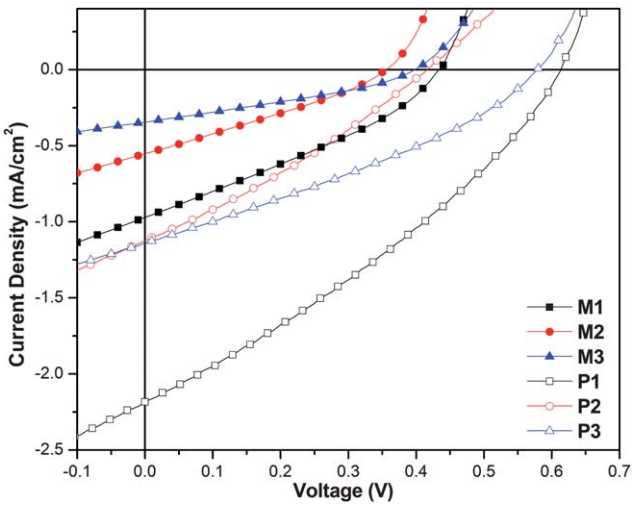

Fig. 6 Current–voltage curves of BHJ solar cells using blended films of **M1–M3** or **P1–P3**:PCBM (1 : 1 w/w) under the illumination of AM 1.5G, 100 mW cm^{-2}.

and $FF = 31.8\%$. It can be seen from Fig. 6 and Table 3 that the devices made from ligands **M1–M3** were limited by low J_{sc} values, which may be due to less creation and dissociation of excitons at the BHJ interfaces followed by transport of free charge carriers towards the collecting electrodes.[28] However, higher J_{sc} values were obtained when the active layers were fabricated from metallo-polymers **P1–P3**. With the similar values of V_{oc} (0.42–0.61 V) and *FF* (30.2–34.1%) in the devices containing metallo-polymers **P1–P3**:PCBM (1 : 1 w/w), it is evident that their variations of PCE values (0.45, 0.14, and 0.22, respectively) were mainly dependent on the J_{sc} values (2.18, 1.14, and 1.14 mA cm^{-2}, respectively). Among PVC devices containing metallo-polymers **P1–P3**, the device containing **P1** exhibited the highest PCE value of 0.45% with J_{sc} (2.18 mA cm^{-2}), V_{oc} (0.61 V), and *FF* (34.1%).

Table 3 Photovoltaic properties of a BHJ solar cell device with a configuration of ITO/PEDOT:PSS/compound:PCBM/Ca/Al[a]

Active layer[b](compound:PCBM)	V_{oc}/V	J_{sc}/mA cm^{-2}	*FF* (%)	PCE (%)
M1	0.43	0.97	31.8	0.13
M2	0.36	0.55	28.8	0.06
M3	0.40	0.34	32.0	0.04
P1	0.61	2.18	34.1	0.45
P2	0.42	1.14	30.2	0.14
P3	0.58	1.14	33.3	0.22

[a] Measured under AM 1.5 irradiation, 100 mW cm^{-2}. [b] Active layer with the weight ratio of Compound:PCBM = 1 : 1.

Among the PVC devices containing metallo-polymers **P1–P3**:PCBM (1 : 1 w/w), **P1** demonstrated a higher J_{sc} values compared to **P2** and **P3**, this could be explained by their EQE curves (see Fig. S10 in the supporting information†). It is evident from the EQE curves that, though all devices exhibited similar EQE values in the short wavelength (*ca.* 400 nm) region but **P1** exhibited higher EQE value at the long wavelength (*ca.* 600 nm) region, this could be the main reason for the higher J_{sc} value of the PVC cell containing **P1**. In BHJ solar cell devices, the absorptions of the long wavelength region are contributed from polymers, and the absorptions in the short wavelength region are mainly from PCBM. The low EQE values in the low-energy absorption bands as well as the high-energy absorption bands in these polymer blends may be due to their poor dissociation of excitons. Therefore, if the EQE values of the devices can be enhanced by increasing the thickness of the active layer without hampering charge separation and transport properties, then the device performances can be improved significantly. Low EQE values can also be observed in some other LBG polymer systems and this problem can be solved by developing new electron acceptor materials.

To the best of our knowledge, compared with all reported heterojunction PVC devices fabricated from terpyridine-containing Ru(II)-metallo-polymers as the active layer,[16] our device containing metallo-polymer **P1** demonstrated the highest PCE value (0.45%), which probably due to the presence of electron donor and acceptor moieties at the core of bis-terpyridyl units in **P1** with the stronger ICT and the broadening of the sensitization range. The reported devices with lower PCE values were because their low V_{oc} values arose from the relatively high HOMO levels, which caused losses due to the limited numbers of photo-generated charges induced by incomplete quasi-Fermi level splittings.[29] To conquer these problems, layer-by-layer (LBL) deposition techniques of Ru(II)-containing polymers with sulfonated polyaniline (SPAN) were utilized, but these techniques were limited by photocurrents.[16b,17a] With polymers as solid polyelectrolytes, Mwaura *et al.* also fabricated LBL devices

View Article Online

Published on 29 November 2010. Downloaded by National Chiao Tung University on 25/04/2014 02:48:02.

by incorporating 50 bilayers of poly(phenylene ethynylene)-based polyanions with cationic C_{60}–NH_3^+ with a total thickness of 50 nm to obtain a maximum PCE value only up to 0.04%.[30] In our case, all the metallo-polymers were in the ideal ranges of HOMO and LUMO to be utilized for BHJ solar cells, so BHJs with **P1–P3** were used to obtain high photocurrents.[31] Compared with the BHJ solar cells fabricated from ionic polythiophene and C_{60},[19] our PVC device made from **P1** exhibited a higher J_{sc} value (2.18 *vs.* 0.97 mA cm^{-2}) with a similar V_{oc} value (0.61 *vs.* 0.67 V), but a similar or little higher PCE value (0.45 *vs.* 0.43) was obtained due to the limited *FF* value (34.1 *vs.* 53%). No significant improvements of PCE values in device performance were observed by changing the PCBM ratio (due to the lower solubility of metallo-polymers **P1–P3** in PCBM compared to DMF). Finally, the device efficiencies of these metallo-polymers are lower than those of neutral polymer-based solar cells, such as P3HT–PCBM, but the highest PCE value of our PVC device containing **P1** is reported among all ionic conjugated polymer-based solar cells so far.

Conclusions

In summary, a series of π-conjugated bis-terpyridyl ligands bearing donor–acceptor units and their corresponding Ru(II)-containing main-chain metallo-polymers were developed and synthesized. The formation of the metallo-polymers were confirmed from the broadened ^{1}H NMR signals, relative viscocity measurements, and UV–vis titration experiments. Apparently, the electro-optical properties of the bis-terpyridyl ligands as well as the metallo-polymers were strongly influenced by the nature of the attached π-conjugated donor–acceptor units and some distinct differences in electro-optical properties were observed between ligands and their analogous metallo-polymers. Because of the broader sensitization of donor–acceptor design in **M1–M3** and **P1–P3**, they exhibited higher J_{sc} values. In addition, owing to the strong intramolecular charge transfers inside the bis-terpyridyl units of **M1–M3** and **P1–P3**, their HOMO levels were tuned to get higher V_{oc} values. An optimum PVC device based on the blended polymer **P1**:PCBM = 1 : 1 (w/w) achieved the PCE value up to 0.45%, with V_{oc} = 0.61 V, J_{sc} = 2.18 mA cm^{-2}, and *FF* = 34.1% (under AM 1.5 G 100 mW cm^{-2}), and those values are comparable with BHJ solar cells fabricated from ionic polythiophene and C_{60}. These metallo-polymers demonstrate a novel family of conjugated polyelectrolytes with the highest PCE value towards potential PVC applications.

Acknowledgements

We express thanks for the financial supports from the National Science Council of Taiwan (ROC) through NSC 97-2221-E-009-008-MY2, National Chiao Tung University through 97W807, and Energy and Environmental Laboratories (charged by Dr Chang-Chung Yang) in Industrial Technology Research Institute (ITRI). We are also grateful to Prof. Tsung Eong Hsieh Department of Materials Science & Engineering, National Chiao Tung University (in Taiwan) for the viscosity measurements and also for their instrumental support.

Notes and references

1 (*a*) J.-M. Lehn, *Supramolecular Chemistry: Concepts and Perspectives* VCH: Weinheim, 1995; (*b*) E. C. Constable, In *Comprehensive Supramolecular Chemistry*, ed. J.-M. Lehn, Pergamon: Elmsford, NY, 1996 Vol. 9, pp 213–252; (*c*) C. J. Jones, *Chem. Soc. Rev.*, 1998, **27**, 289–300; (*d*) M. Elhabiri and A.-M. Elbrecht-Gary, *Coord. Chem. Rev.*, 2008, **252**, 1079–1092.
2 (*a*) B. Song, G. Wang, M. Tan and J. Yuan, *J. Am. Chem. Soc.*, 2006, **128**, 13442–13450; (*b*) J. Hovinen and H. Hakala, *Org. Lett.*, 2001, **3**, 2473–2476.
3 (*a*) U. Kolb, K. Buscher, C. A. Helm, A. Lindner, A. F. Thunemann, M. Menzel, M. Higuchi and D. G. Kurth, *Proc. Natl. Acad. Sci. U. S. A.*, 2006, **103**, 10202–10206; (*b*) M. Oh and C. A. Mirkin, *Nature*, 2005, **438**, 651–654; (*c*) D. G. Kurth and M. Higuchi, *Soft Matter*, 2006, **2**, 915–927.
4 (*a*) W. S. Huang, Y. H. Wu, Y. C. Hsu, H. C. Lin and J. T. Lin, *Polymer*, 2009, **50**, 5945–5958; (*b*) W. S. Huang, C. W. Lin, J. T. Lin, J. S. Huang, C. W. Chu, Y. H. Wu and H. C. Lin, *Org. Electron.*, 2009, **10**, 594–606; (*c*) M. Yoshizawa, M. Tamura and M. Fujita, *Science*, 2006, **312**, 251–254; (*d*) O. Mamula and A. von Zelewsky, *Coord. Chem. Rev.*, 2003, **242**, 87–95; (*e*) M. Barboiu, G. Vaughan, R. Graff and J.-M. Lehn, *J. Am. Chem. Soc.*, 2003, **125**, 10257–10265.
5 (*a*) K. D. Oyler, F. J. Coughlin and S. Bernhard, *J. Am. Chem. Soc.*, 2007, **129**, 210–217; (*b*) S. Graber, K. Doyle, M. Neuburger, C. E. Housecroft, E. C. Constable, R. D. Costa, E. Orti, D. Repetto and H. J. Bolink, *J. Am. Chem. Soc.*, 2008, **130**, 14944–14945; (*c*) A. Maier, A. R. Rabindranath and B. Tieke, *Chem. Mater.*, 2009, **21**, 3668–3676; (*d*) E. Holder, B. M. W. Langeveld and U. S. Schubert, *Adv. Mater.*, 2005, **17**, 1109–1121; (*e*) T. Bessho, E. C. Constable, M. Graetzel, A. H. Redondo, C. E. Housecroft, W. Kylberg, M. K. Nazeeruddin, M. Neuburger and S. Schaffner, *Chem. Commun.*, 2008, 3717–3719; (*f*) M. Ruben, A. Landa, E. Lortscher, H. Riel, M. Mayor, H. Gorls, H. B. Weber, A. Arnold and F. Evers, *Small*, 2008, **4**, 2229–2235.
6 (*a*) U. S. Schubert, H. Hofmeier and G. R. Newkome, *Modern Terpyridine Chemistry* Wiley-VCH: Weinheim, 2006; (*b*) E. C. Constable, *Chem. Soc. Rev.*, 2007, **36**, 246–253; (*c*) E. Medlycott and G. S. Hanan, *Chem. Soc. Rev.*, 2005, **34**, 133–142; (*d*) N. Miyashita and D. G. Kurth, *J. Mater. Chem.*, 2008, **18**, 2636–2649.
7 (*a*) M. Jäger, L. Eriksson, J. Bergquist and O. Johansson, *J. Org. Chem.*, 2007, **72**, 10227–10230; (*b*) A. Winter, D. A. Egbe and U. S. Schubert, *Org. Lett.*, 2007, **9**, 2345–2348; (*c*) K. Seo, A. V. Konchenko, J. Lee, G. S. Bang and H. Lee, *J. Mater. Chem.*, 2009, **19**, 7617–7624; (*d*) M. Schmittel, V. Kalsani, P. Mal and J. W. Bats, *Inorg. Chem.*, 2006, **45**, 6370–6377; (*e*) S. C. Yuan, H. B. Chen and J. Pei, *Org. Lett.*, 2006, **8**, 5701–5704; (*f*) E. C. Constable, E. Figgemeier, C. E. Housecroft, S. L. Kokatam, E. A. Medlycott, M. Neuburger, S. Schaffner and A. Zampese, *Dalton Trans.*, 2008, 6752–6762; (*g*) M. W. Cooke and G. S. Hanan, *Chem. Soc. Rev.*, 2007, **36**, 1466–1476.
8 (*a*) A. Benniston, A. Harriman, P. Li, P. V. Patel and C. A. Sams, *J. Org. Chem.*, 2006, **71**, 3481–3493; (*b*) M. W. Cooke, G. S. Hanan, F. Loiseau, S. Campagna, M. Watanabe and Y. Tanaka, *J. Am. Chem. Soc.*, 2007, **129**, 10479–10488; (*c*) X. Chen, Q. Zhou, Y. Cheng, Y. Geng, D. Ma, Z. Xie and L. Wang, *J. Lumin.*, 2007, **126**, 81–90; (*d*) F. Camerel, R. Ziessel, B. Donnio, C. Bourgogne, D. Guillon, M. Schmutz, C. Iacovita and J. P. Bucher, *Angew. Chem., Int. Ed.*, 2007, **46**, 2659–2662; (*e*) K. Sénéchal-David, J. P. Leonard, S. E. Plush and T. Gunnlaugsson, *Org. Lett.*, 2006, **8**, 2727–2730.
9 (*a*) S. Vaduvescu and P. G. Potvin, *Eur. J. Inorg. Chem.*, 2004, 1763–1769; (*b*) R. Dobrawa and F. Wrthner, *J. Polym. Sci., Part A: Polym. Chem.*, 2005, **43**, 4981–4995; (*c*) A. Winter, C. Friebe, M. D. Hager and U. S. Schubert, *Macromol. Rapid Commun.*, 2008, **29**, 1679–1686; (*d*) J. P. Sauvage, J. P. Collin, J. C. Chambron, S. Guillerez, C. Coudret, V. Balzani, F. Barigelletti, L. Decola and L. Flamigni, *Chem. Rev.*, 1994, **94**, 993–1019; (*e*) F. S. Han, M. Higuchi, T. Ikeda, Y. Negishi, T. Tsukuda and D. G. Kurth, *J. Mater. Chem.*, 2008, **18**, 4555–4560.
10 E. C. Constable and A. M. W. C. Thompson, *J. Chem. Soc., Chem. Commun.*, 1992, 617–619.

 This journal is © The Royal Society of Chemistry 2011

View Article Online

Published on 29 November 2010. Downloaded by National Chiao Tung University on 25/04/2014 02:48:02.

11 (*a*) G. R. Newkome, E. He and C. N. Moorefield, *Chem. Rev.*, 1999, **99**, 1689–1746; (*b*) A. H. Flood, J. F. Stoddart, D. W. Steuerman and J. R. Heath, *Science*, 2004, **306**, 2055–2056; (*c*) P. R. Andres and U. S. Schubert, *Adv. Mater.*, 2004, **16**, 1043–1068; (*d*) I. Ciofini, P. P. Lainé, F. Bedioui and C. Adamo, *J. Am. Chem. Soc.*, 2004, **126**, 10763–10777; (*e*) H. Hofmeier and U. S. Schubert, *Chem. Soc. Rev.*, 2004, **33**, 373–399; (*f*) A. Winter, C. Friebe, M. Chiper, M. D. Hager and U. S. Schubert, *J. Polym. Sci., Part A: Polym. Chem.*, 2009, **47**, 4083–4098.

12 (*a*) G. Bianké and R. Häner, *Chem. Bio. Chem.*, 2004, **5**, 1063–1068; (*b*) C. N. Carlson, C. J. Kuehl, R. E. Da-Re, J. M. Veauthier, E. J. Schelter, A. E. Milligan, B. L. Scott, E. D. Bauer, J. D. Thompson, E. D. Morris and K. D. John, *J. Am. Chem. Soc.*, 2006, **128**, 7230–7241; (*c*) P. P. Lainé, F. Bedioui, F. Louiseau, C. Chiorboli and S. Campagna, *J. Am. Chem. Soc.*, 2006, **128**, 7510–7521; (*d*) P. Coppo, M. Duati, V. N. Kozhevnikov, J. W. Hofstraat and L. De Cola, *Angew. Chem., Int. Ed.*, 2005, **44**, 1806–1810; (*e*) A. Barbieri, B. Ventura, F. Barigeletti, A. de Nicolar, M. Quesada and R. Ziessel, *Inorg. Chem.*, 2004, **43**, 7359–7368.

13 (*a*) H. Hofmeier and U. S. Schubert, *Chem. Commun.*, 2005, 2423–2432; (*b*) F. Barigeletti, L. Flamigni, V. Balzani, J.-P. Collin, J.-P. Sauvage, A. Sour, E. C. Constable and A. M. W. Cargill Thompson, *J. Am. Chem. Soc.*, 1994, **116**, 7692–7699; (*c*) D. H. Xu, L. L. Hawk, D. M. Loveless, S. L. Jeon and S. L. Craig, *Macromolecules*, 2010, **43**, 3556–3565; (*d*) G. Schwarz, Y. Bodenthin, T. Geue, J. Koetz and D. G. Kurth, *Macromolecules*, 2010, **43**, 494–500; (*e*) S. Kelch and M. Rehahn, *Macromolecules*, 1999, **32**, 5818–5828.

14 (*a*) F. Schlutter, A. Wild, A. Winter, M. D. Hager, A. Baumgaertel, C. Friebe and U. S. Schubert, *Macromolecules*, 2010, **43**, 2759–2771; (*b*) R. Dobrawa, M. Lysetska, P. Ballester, M. Grüne and F. Würthner, *Macromolecules*, 2005, **38**, 1315–1325; (*c*) S.-H. Hwang, C. N. Moorefield, P. Wang, J.-Y. Kim, S.-W. Lee and G. R. Newkome, *Inorg. Chim. Acta*, 2007, **360**, 1780–1784; (*d*) A. Winter, C. Friebe, M. Chiper, U. S. Schubert, M. Presselt, B. Dietzek, M. Schmitt and J. Popp, *Chem. Phys. Chem.*, 2009, **10**, 787–798.

15 (*a*) Y. Y. Chen and H. C. Lin, *J. Polym. Sci., Part A: Polym. Chem.*, 2007, **45**, 3243–3255; (*b*) Y. Y. Chen, Y. T. Tao and H. C. Lin, *Macromolecules*, 2006, **39**, 8559–8566; (*c*) Y. Y. Chen and H. C. Lin, *Polymer*, 2007, **48**, 5268–5278.

16 (*a*) K. W. Cheng, C. S. C. Mak, W. K. Chan, A. M. C. Ng and A. B. Djurii, *J. Polym. Sci., Part A: Polym. Chem.*, 2008, **46**, 1305–1317; (*b*) K. K. Y. Man, H. L. Wong, W. K. Chan, C. Y. Kwong and A. B. Djurisic, *Chem. Mater.*, 2004, **16**, 365–367; (*c*) P. D. Vellis, J. A. Mikroyannidis, C. N. Lo and C. S. Hsu, *J. Polym. Sci., Part A: Polym. Chem.*, 2008, **46**, 7702–7712; (*d*) V. Duprez, M. Biancardo, H. Spanggaard and F. C. Krebs, *Macromolecules*, 2005, **38**, 10436–10448; (*e*) O. Hagemann, M. Jørgensen and F. C. Krebs, *J. Org. Chem.*, 2006, **71**, 5546–5559.

17 (*a*) K. K. Y. Man, H. L. Wong, W. K. Chan, A. B. Djurisic, E. Beach and S. Rozeveld, *Langmuir*, 2006, **22**, 3368–3375; (*b*) Y. Pan, B. Tong, J. Shi, W. Zhao, J. Shen, J. Zhi and Y. Dong, *J. Phys. Chem. C*, 2010, **114**, 8040–8047; (*c*) V. Stepanenko, M. Stocker, P. Müller, M. Büchner and F. Würthner, *J. Mater. Chem.*, 2009, **19**, 6816–6826.

18 M. Gratzel, *Nature*, 2001, **414**, 338–344.

19 (*a*) J. Yang, A. Garcia and T. Q. Nguyen, *Appl. Phys. Lett.*, 2007, **90**, 103514; (*b*) C. V. Hoven, A. Garcia, G. C. Bazan and T. Q. Nguyen, *Adv. Mater.*, 2008, **20**, 3793–3810.

20 M. Schmelz and M. Rehahn, *e-Polym.*, 2002, **47**, 1–29.

21 B. Hu, A. Fuchs, S. Huseyi and F. Gordaninejad, *J. Appl. Polym. Sci.*, 2006, **100**, 2464–2479.

22 (*a*) X. Y. Wang, A. D. Guerzo and R. H. Schmehl, *Chem. Commun.*, 2002, 2344–2345; (*b*) H. Hofmeier, A. El-ghayoury, A. P. H. J. Shenning and U. S. Schubert, *Chem. Commun.*, 2004, 318–319.

23 (*a*) F. Schlutter, A. Wild, A. Winter, M. D. Hager, A. Baumgaertel, C. Friebe and U. S. Schubert, *Macromolecules*, 2010, **43**, 2759–2771; (*b*) A. Winter, C. Friebe, M. D. Hager and U. S. Schubert, *Eur. J. Org. Chem.*, 2009, 801–809; (*c*) G. Schwarz, T. K. Sievers, Y. Bodenthin, I. Hasslauer, T. Geue, J. Koetz and D. G. Kurth, *J. Mater. Chem.*, 2010, **20**, 4142–4148.

24 (*a*) N. Blouin, A. Michaud, D. Gendron, S. Wakim, E. Blair, R. N. Plesu, M. Bellette, G. Durocher, Y. Tao and M. Leclerc, *J. Am. Chem. Soc.*, 2008, **130**, 732–742; (*b*) H. X. Zhou, L. Q. Yang, S. Q. Xiao, S. B. Liu and W. You, *Macromolecules*, 2010, **43**, 811–820; (*c*) H. Padhy, J. H. Huang, D. Sahu, D. Patra, D. Kekuda, C. W. Chu and H. C. Lin, *J. Polym. Sci. Part A: Polym. Chem.*, 2010, **48**, 4823–4834.

25 (*a*) D. Oyama, M. Kido, A. Orita and T. Takase, *Polyhedron*, 2010, **29**, 1337–1343; (*b*) Q. X. Zhou, W. H. Lei, C. Li, Y. J. Hou, X. S. Wang and B. W. Zhang, *New J. Chem.*, 2010, **34**, 137–140.

26 (*a*) S. Flores-Torres, G. R. Hutchison, L. J. Soltzberg and H. D. Abruna, *J. Am. Chem. Soc.*, 2006, **128**, 1513–1522; (*b*) D. Oyama, M. Kido, A. Orita and T. Takase, *Polyhedron*, 2010, **29**, 1337–1343.

27 B. Schulze, C. Friebe, M. D. Hager, A. Winter, R. Hoogenboom, H. Gorls and U. S. Schubert, *Dalton Trans.*, 2009, 787–797.

28 P. W. M. Blom, V. D. Mihailetchi, L. J. A. Koster and D. E. Markov, *Adv. Mater.*, 2007, **19**, 1551–1566.

29 L. J. A. Koster, V. D. Mihailetchi, R. Ramaker and P. W. M. Blom, *Appl. Phys. Lett.*, 2005, **86**, 123509.

30 J. K. Mwaura, M. R. Pinto, D. Witker, N. Ananthakrishnan, K. S. Schanze and J. R. Reynolds, *Langmuir*, 2005, **21**, 10119–10126.

31 M. Hiramoto, H. Fujiwara and M. Yokoyama, *J. Appl. Phys.*, 1992, **72**, 3781.